Nonstationarity of AGN variability: The only way is down!

Neven Caplar [ID],[1] Theodore Penna,[2] and Sean Johnson [ID][1]

[1]*Department of Astrophysical Sciences, Princeton University, 4 Ivy Ln., Princeton, NJ 08544, USA*
[2]*Department of Physics and Astronomy, Tufts University, Medford, MA 02155, USA*

ABSTRACT

To gain insights into long-term Active Galactic Nuclei (AGN) variability, we analyze an AGN sample from the Sloan Digital Sky Survey (SDSS) and compare their photometry with observations from Hyper Suprime-Cam survey (HSC) observed $< 14.85 >$ years after SDSS. On average, the AGN are fainter in HSC than SDSS. We demonstrate that the difference is not due to subtle differences in the SDSS versus HSC filters or photometry. The decrease in mean brightness is redshift dependent, consistent with expectations from cosmological time dilation. Moreover, the mean decrease in brightness is stronger for more luminous AGN, and for objects with longer time separation between measurements. We demonstrate that the measured mean brightness decrease and dependence on redshift and Eddington ratio is consistent with simple models of AGN variability on long (Myr, Gyr) timescales. Our results can therefore be used to constrain demographic properties of AGN population. Finally, we note that the mean decrease in brightness violates the stationarity assumption often invoked in AGN variability studies.

Keywords: accretion, accretion disks - black hole physics - methods: data analysis - quasars: general

1. INTRODUCTION

Change of brightness of AGN with time is one of its most ubiquitous properties. The fluctuations of AGN luminosity, i.e., AGN variability, have been directly observationally studied in large samples on timescale of minutes, days, years and decades (e.g., MacLeod et al. 2010, 2012; Morganson et al. 2014; Cartier et al. 2015; Caplar et al. 2017; Smith et al. 2018). These studies enable us to explore physics of AGN on the scales which are completely inaccessible with any other methods for the vast majority of these objects. Through indirect methods and simulations the AGN variability has also been studied on Myr and Gyr scales (e.g., Novak et al. 2011; Bland-Hawthorn et al. 2013; Sartori et al. 2018).

Most of the direct observational studies mentioned above concentrated on studying the variability as a weakly stationary process i.e., with the assumption that the mean luminosity of statistically big enough ensemble of AGN does not change with time. The AGN variability is then usually characterized by computation of structure function or similar quantity as a function of time, i.e., by specifying variance of the measured observations separated by a given time interval. Empirically, stochastic variability measured in these studies dominated any possible subtle changes in the mean brightness. From theoretical grounds, the stochastic variability is thought to be reflective of the details of the physic of accretion disk and other nearby structure, while the mean change of luminosity would be more connected with long-scale accretion processes which should have minimal impact on timescale of typical surveys (Lawrence 2018).

The assumption of stationarity on short timescales differs from the long term studies of AGN activity, which indicate large changes in AGN activity on Myr and Gyr scales. The firmest observational proof comes from the studies of individual "Voorwerp" objects (e.g., Sartori et al. 2016), which clearly show that, at least some, AGN exhibit changes in their luminosity of the orders of tens of magnitudes on these timescales though most? AGN

Corresponding author: Neven Caplar
ncaplar@princeton.edu

exhibit minimal changes over $\approx 3 \times 10^5$ years Johnson et al. (2018).

There has been comparatively little observational research on the deviations from the assumed stationary and symmetric behaviour of AGN variability. Number of early studies conducted observationally difficult searches for potential difference in the variability properties when AGN get brighter or dimmer (de Vries et al. 2003, 2005; Bauer et al. 2009; Voevodkin 2011), but found little or no evidence for deviations from full symmetry. MacLeod et al. (2012) combined the earliest statistically significant sample of AGN measurements from the Palomar Observatory Sky Surveys (POSS) with the SDSS data. They noted that objects from POSS are brighter in the earlier survey and dimmer when observed in SDSS. They noted the existence of " Malmquist-like" bias, i.e., some of the object are not available in both of the surveys, because their luminosity has changed enough so that they drop below the luminosity limit. It is noted that this does not necessarily imply that there is change of the mean brightness of a sample, because even if the mean brightness of an ensemble stays the same, if the variability is strong enough, some of the objects will drop below sensitivity limit of any survey. Morganson et al. (2014) also found the decrease of the mean brightness on decadal scale, for the sample of AGN from the SDSS observed in Pan-STARRS1, but attributed this effect to filter differences.

Here, we use the AGN sample from SDSS and measure their mean brightness in SDSS and HSC. In this work we aim show that AGN exhibit changes in their mean brightness on the timescales accessible with past (SDSS) and current (HSC) surveys.

The code, the data and additional examples are available at github.com/nevencaplar/Nonstationarity.

2. OBSERVATIONS

2.1. Data

To study AGN variability on decadal timescales, we identified AGN from the SDSS DR7 Quasar catalog Schneider et al. (2010) that were also observed later by the Hyper Suprime-Cam (HSC; Miyazaki et al. 2018) Subaru Strategic imaging survey. The SDSS survey used dedicated 2.5-m (Gunn et al. 2006) telescope at Apache Point Observatory and obtained images in 5 optical bands (ugriz) over large patch ($\sim$10000 deg^2) of Northern sky. For presentation of the photometric calibration and selection function of objects we refer the reader to detailed discussion in Schneider et al. (2010). The HSC survey is a wide-field optical imaging program conducted with 8.2 meter Subaru telescope. The second data release, that was made available in May 2019,

covers around 300 deg^2 overlapping with the SDSS footprint. The data in 5 optical bands (grizy) is available down to around 26 magnitude. This great depth is especially beneficial for this work, as it is virtually impossible for the AGN from the SDSS sample to drop below the luminosity limit of the HSC survey. Full details of the HSC survey are available in the release paper by Aihara et al. (2019).

We searched for objects from SDSS AGN catalog in the HSC data and record their g, r and i psf-magnitudes We have excluded all of the objects with any flags showing problems in the calibration. This conservative cut ensures that our conclusions are not driven by possible problems in the brightness measurements in the HSC pipeline. This procedure yields 5919 matched AGN found in both surveys.

2.2. Main result

We proceed to measure the difference in the brightness between the two surveys. We split the sample in bins of redshift, where each bin consist of 100 objects. This number enables us to follow the redshift evolution of the trends in some detail, while keeping the uncertainty on the mean brightness change relatively low. We then, for each redshift bin, deduce the mean and the median difference between the observed psf-magnitude in SDSS and HSC surveys.

We present our result in Figure 1. To avoid cluttering the plot we only explicitly show data points at each redshift for measurements in the g-band. The uncertainties on the mean value at each redshift have been derived by bootstraping the underlying 100 AGN in each bin. We choose to present g-band result given that contribution of the host-galaxy light, however small for these bright quasars, will be smallest in the bluest available band. However, results for all 3 bands are very similar. We also show linear fits to the data in all 3 bands, where one can explicitly see the similarity between all of the results. We have also verified that the redshift evolution effect is present if we use median differences instead of mean differences of magnitudes, but the magnitude of the effect is somewhat decreased. For instance, the best fit for the median difference is $-0.139 + 0.051z$ while for mean difference it is $-0.176 + 0.06z$. The fact the effect is still present when using the median shows that the effect can not fully explained by relatively small number of extremely variable quasars (e.g., MacLeod et al. 2016; Rumbaugh et al. 2018). We believe that the difference is consistent with the model in which measured changes of the mean/median flux are the consequence of the long-term AGN behaviour. We therefore also show the linear fit as a function of restframe time sep-
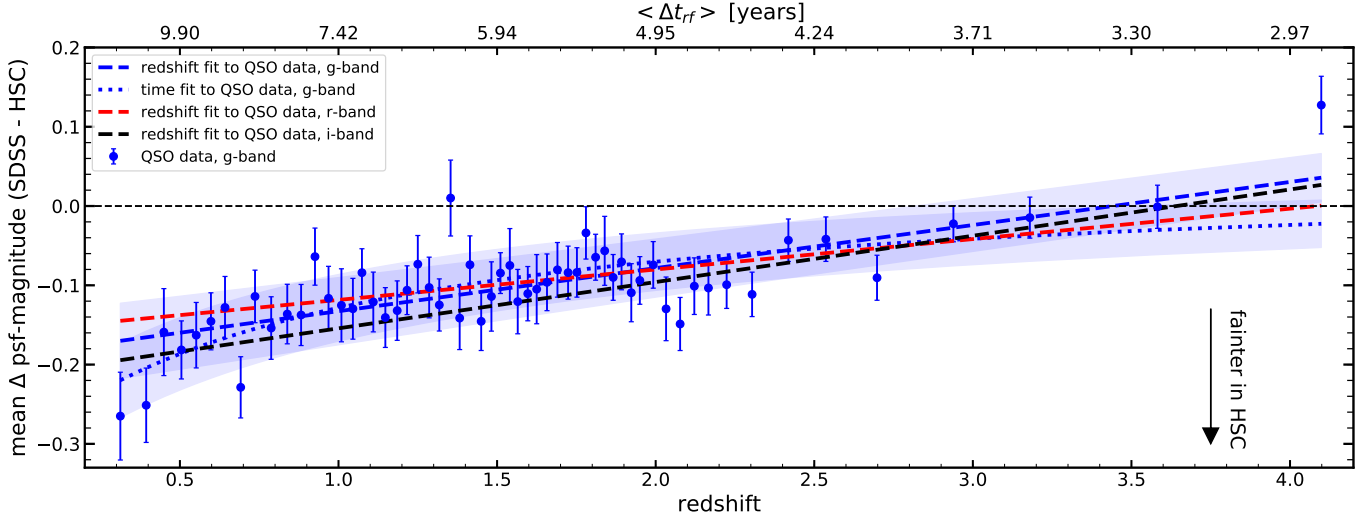
Figure 1. Mean difference in the measured psf-magnitudes for the sample of AGN from SDSS that have been observed in both SDSS and HSC. Blue points shows the data for the g-band, while the blue dashed line and the shaded region show the linear fit as function of redshift to the data and 1-σ uncertainty. The red and the black dashed lines and the associated shaded regions show linear fit and 1-σ uncertainty for the data in r- and i- bands, respectively. The dotted line show fit as a function of restframe time-separation between measurements, indicated on the upper axis.

aration between two measurements, i.e., as a function of 14.85 years/$(1 + z)$, which also provides good explanation for the observed data. We discuss the proposed model further in Section 3.

In order to make sure that observed redshift dependence is the real physical effect, and not a spurious effect due to differences between two surveys, we conduct four different checks which we list here:

- consideration of filter differences

- constructing the control sample

- separating the AGN sample according to brightness

- separating the AGN sample according to the time separation

We elaborate on each of these procedures in some detail below. For consistency, we always show results for mean difference in g-band and conduct linear fits as a function of redshift, but all of conclusion are applicable to all 3 bands and fitting variables (redshift or restframe time separation).

2.3. *Filter difference and control sample*

We performed two experiments to assess the potential impact of differences in the photometry between the SDSS and HSC surveys which could lead to spurious apparent variability. First, to assess the potential impact of differences in the filter systems on the measured magnitudes, we predicted $g_{\mathrm{SDSS}} - g_{\mathrm{HSC}}$ for the mean SDSS

quasar SED (Vanden Berk et al. 2001) as a function of redshift using the SDSS (Fukugita et al. 1996) and HSC (Kawanomoto et al. 2018) defined system throughput including the filter, telescope, camera, and the survey standard atmospheres. Second, we constructed a control sample of "fake AGN" consisting of non-variable stars with similar colors as the AGN. The stars were taken from the catalog of non-variable objects from the equatorial Stripe 82 presented in Ivezić et al. (2007) which we additionally cleaned by removing suspected AGN from Flesch (2015). For each AGN we find the star which minimizes the euclidean distance between the measured values of g-, r- and i- bands in SDSS. After that, we treat the catalog of stars that we have created in exactly the same way as we have treated the AGN sample. As, by definition, we expect no change in the brightness of these stars when imaged in the two surveys, any systematic differences between two surveys will be expressed in this comparison. These experiments capture effects both from filter differences and from any differences in the PSF magnitude measurement techniques.

We show the results of this experiment and deduce effects of filter differences in 2. We see the large difference between the control sample of matched stars and the sample of AGN. We emphasize the absence of "redshift" trend in the control sample. This is an expected result, as the different "redshift" for the control sample correspond to only relatively small changes in the mean color of the objects, which does not affect the calibration of the surveys greatly. We also note how the expected filter differences between the two surveys pro-
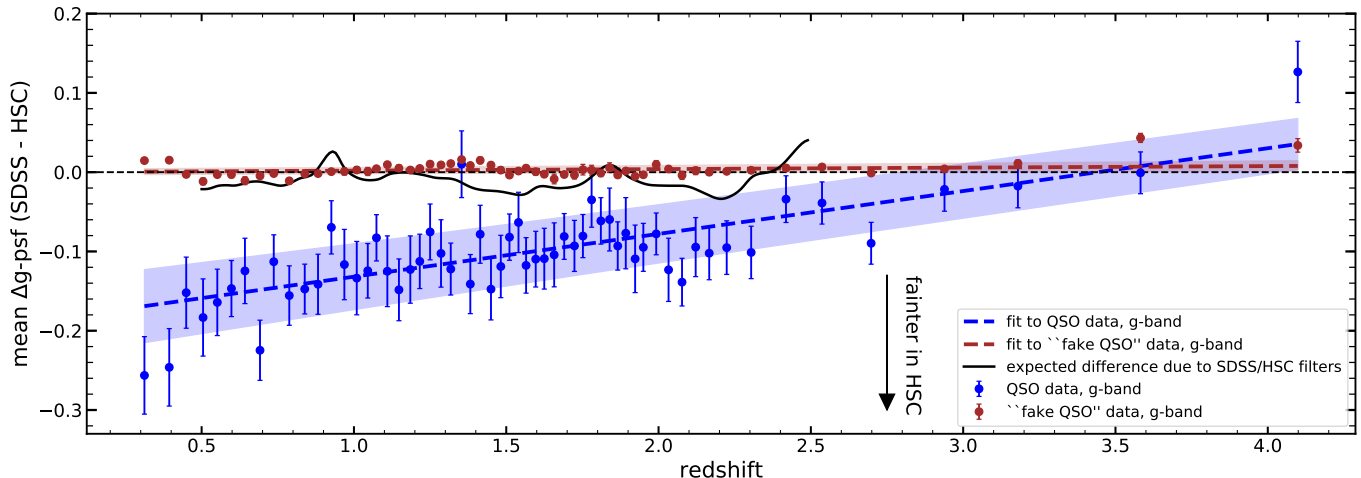
Figure 2. Mean difference in the measured psf-magnitudes for the sample of AGN from SDSS, and the sample of stars that match theses AGN in color. Blue points shows the data for AGN in, while the blue line and the shaded region show the linear fit to the data and 1-σ uncertainty. This is equivalent to the data and fit shown in Figure 1. Maroon points, line and the shaded region show equivalent quantities constructed for the sample of non-variable stars in Stripe 82 region. Black line shows the expected redshift dependence due to filter differences between two surveys.

duce relatively small and almost redshift-independent effect. This is due to the small differences between the SDSS (Fukugita et al. 1996) and HSC (Kawanomoto et al. 2018) g-bands,[1] and characteristic power-law SED of a AGN which result in modest $u - g$ and $g - r$ colors of ≈ -0.2 to 0.3 on the AB system (e.g. Richards et al. 2001). Based on these two tests, we conclude that differences in the survey photometry cannot explain the observed difference between two AGN measurements.

2.4. *Split according to brightness*

We then proceed to study the redshift effect after splitting our sample in brightness. We do this for two separate reasons. Obsessionally, we would expect that systematic differences between the surveys would be more strongly manifested for objects that have lower brightness, as various errors and uncertainties start to dominate closer to the brightness limit of SDSS survey. Also, even though the starting sample is the sample of bright quasars, at lower redshift and lower luminosities the galaxy contribution may start to be non-negligible (Shen et al. 2011), which might bias our results. On the other hand, physically, we would expect that the mean brightness change would be larger for brighter AGN, as those AGN are, on average, first imaged in more extreme parts of their life-cycle and we would therefore expect that they will drop more during any given observed timeframe.

We have split the data in each redshift bin in 5 further bins, according to their observed brightness. We then proceed to fit the data in each of these brightness bins with a linear function and show the results of the fitting procedure in Figure 3. As errors on the fit are very similar for all of the 5 bins, we show the mean error on the fit in the separate panel below the main panel. We see that the effect is indeed stronger for the brighter AGN, as we expected from both observational and physical grounds. This makes us even more confident in the physical nature of this effect. We also wish to point out that the raise above zero for the dimmest objects is mostly driven by the few last points at the highest redshifts and it is not obvious that is also a physical result.

2.5. *Split according to the time separation*

As a final check we want to separate our sample in the bins according to the time-separation between the observations. As both surveys took data over several years, we can look at the data that has been taken, by random chance, at shortest and longest time intervals and compare the results. If the change of mean brightness is mostly due to observational effects we would expect no difference between the short and long separation datasets, while if the difference is physical we would expected to see some difference between these two sets.

This experiment is somewhat complicated by the fact that we, at this stage, are only working with the stacked HSC data, i.e., the measured brightness of any object is a combination of measurements at different times during the duration of the survey. For HSC data we take

---

[1] with $\lambda_{\rm eff} = 4770$ Å and FWHM $= 1379$ Å for SDSS versus $\lambda_{\rm eff} = 4754$ Å and FWHM $= 1395$ Å for HSC
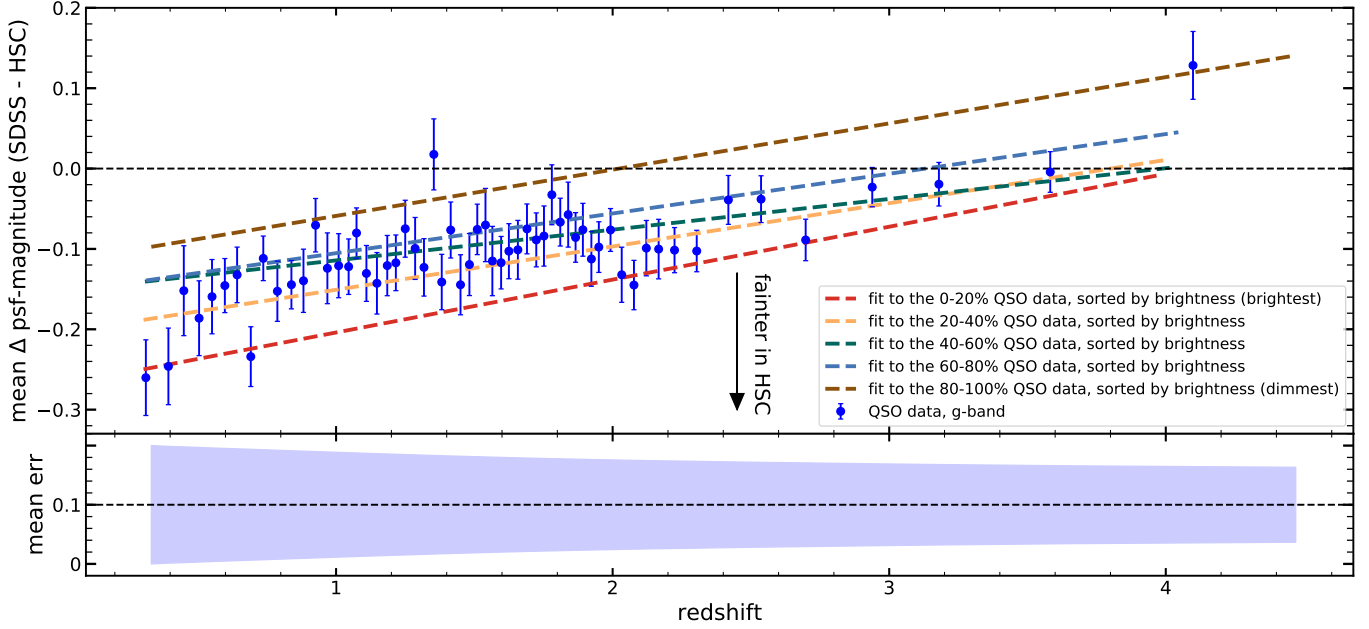
Figure 3. Mean difference in the measured psf-magnitudes in g-band for the sample of AGN separated according to their brightness at each redshift. The blue data shows the data for the whole sample and is the same as in Figure 1. Differently colored lines shows the result of the linear fit to the subsets of the data, that have been constructed by separating the data at each redshift in quantiles, according to their brightness. Lower panel shows the mean error on these linear fits, which is very similar for all of the subsets.

mean of all of the observation times that go into each stacked observation, and use that "mean time" as the time of the observation. The distribution of time differences between the surveys is roughly normal, with the mean at 14.85 years. We then create a sample out of the data for which the time separation is within 20% of the shortest time separations (short separation sample) and out of the data which is has time separation which is within 20% of the longest time separations (long separation sample). Mean time separation for the short separation sample is 12.94 years, and for the long separation sample is 16.89 years.

We then proceed as before and study the redshift dependence of each of these samples. We have binned the data in coarser redshift bins in order to preserve statistical power of individual data, given that each of the subsamples contains a fraction of the full data. We show the data, the results of the linear fit to the full data and long/short separations at Figure 4. We see that, in general, long separation data does indeed tend to show larger changes between two surveys. Of course, the results are noisy, which is not unsurprising given the underlying stochastic variability. We also emphasize that given the relatively small differences in the time separation between long and short separation samples the expected differences are also small. In Figure 4 we also show the expected linear fit for the short separation sample, which was derived from the long sep-

aration sample by multiplying the slope with the ratio of mean time separations of each sample i.e., with the factor 12.94/16.89. This is a simplified assumption, as mean change of brightness are not necessarily linear with time, but we see that the modifications explains well the magnitude of the observed difference.

3. MODELLING AND DISCUSSION

In this section we wish to indicate to the reader how this effect can be used to constraint parameters of AGN accretion, given the reasonable set of assumptions. Recently Sartori et al. (2019) developed the code which is capable of simulating Eddington ratio-curves with the duration of Myr to Gyr, and the time resolution of 10-100 days. The inputs to the code are probability density function (PDF; in this case this is the Eddington ratio function) and the power spectrum density (PSD). We model the PSD as a broken power, i.e., with

$$PSD(f) = A \times \left[\left(\frac{f}{f_{\mathrm{br}}} \right)^{\alpha_{\mathrm{low}}} + \left(\frac{f}{f_{\mathrm{br}}} \right)^{\alpha_{\mathrm{high}}} \right]^{-1} \quad (1)$$

where f_{br} is the break frequency, and α_{low} and α_{high} are the slopes at lower and higher frequencies, respectively (longer and shorter timescales, respectively). While there is agreement in the community that $\alpha_{\mathrm{high}} \approx 2$ (except perhaps at shortest scales, <10 days, e.g., Edelson et al. (2014)), the deduced values for α_{low} and f_{br} vary greatly depending on the survey and method used
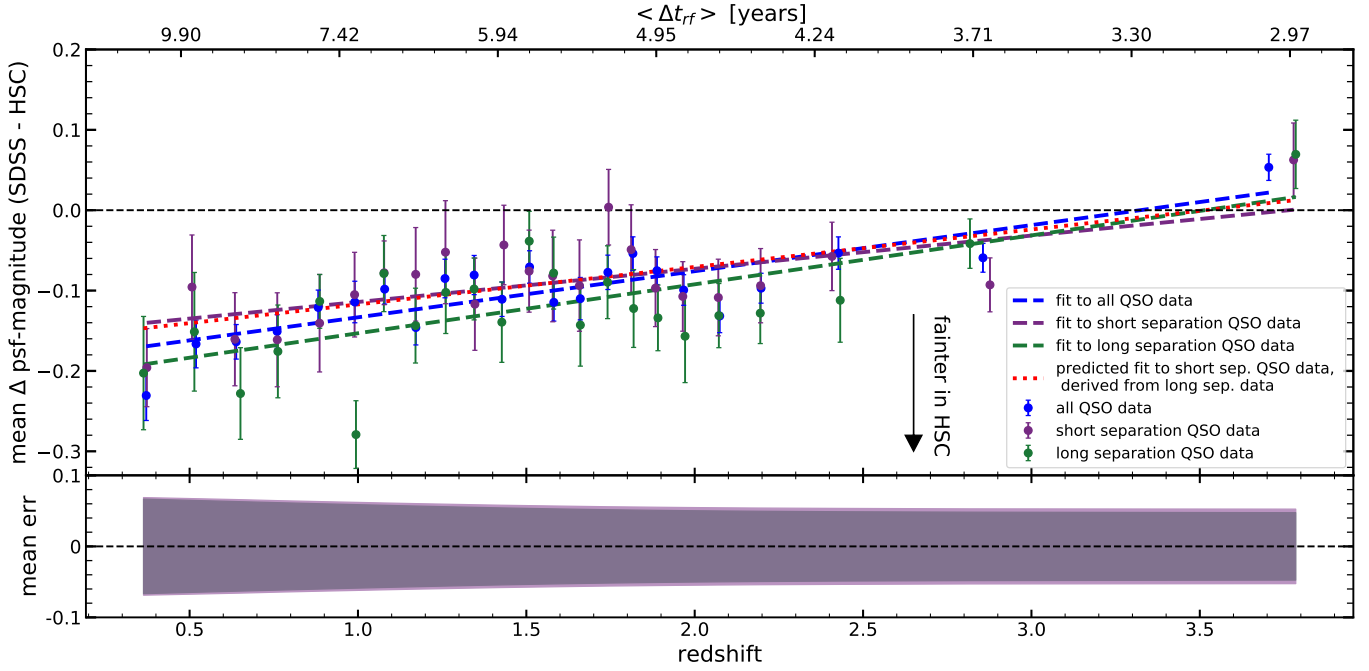
Figure 4.   Mean difference in the measured psf-magnitudes in g-band for the sample of AGN split according to the time separation between the measurements. Blue points shows the data for the whole sample of AGN in the g-band, while the blue line shows the linear fit to the data. This is equivalent to the data and fit shown in Figure 1, although the binning is different to match binning for short and long separation samples (shown in magenta and green, respectively). Red dotted line shows the simplest "derivation" of the short separation fit, which has been derived from the long separation fit and reduced by the ratio of the mean time-separations for these two samples (12.94, 16.89 years). Lower panel shows the error on the linear fit for the short and long separation data.
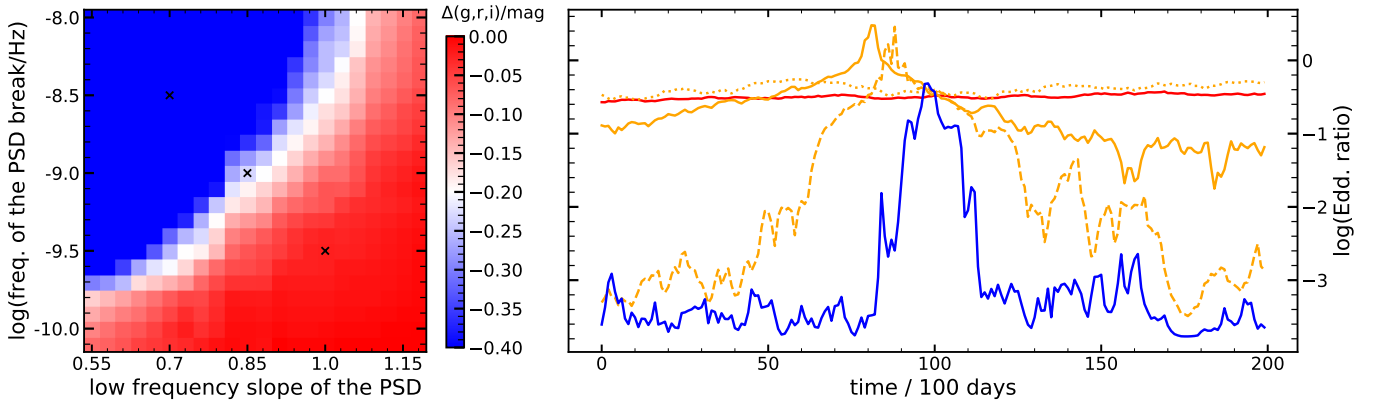
Figure 5. *Left:* The mean change in measured brightness for AGN sampled at 0.5 mag above the brightness cut of a hypothetical survey, and measured again 14.85 years later, as a function of α_{low} and f_{br}. *Right:* Typical "light curves" (Eddington ratio) curves, from each of the areas denoted with a small cross on the left hand side. Colors correspond to the colors on the left hand side, where we use orange (instead of white) to color the curves from the middle, observationally plausible, region. We show three curves from the middle region to demonstrate the diversity of behaviours.

(e.g., MacLeod et al. 2010, 2012; Graham et al. 2014; Kozłowski 2017). Physically, the determination of f_{br} is of great interest as it would be able to provide us with a clue about the physical scale on which the properties of AGN accretion change.

In left panel of Figure 5 we show the expected mean change of the measured brightness during 14.85 years, the average time difference between two measurements, as a function of f_{br} and α_{low}. This plot has been done for the systems that are selected at Eddington ratio which is 0.2 dex (0.5 mag) above the break of the Eddington ratio distributions, which mimics the SDSS observational cut. We can see the observation of mean brightness change defines very specific range of allowed values in this parameter space. The two parameters are somewhat degenerate - observationally there is little difference is the process decorrelates very strongly at longer timescale (small α_{low} and large f_{br}) or wealky at shorter timescales (large α_{low} and small f_{br} - see also Figure 12. in Caplar & Tacchella 2019). On the right hand side of 5 we show representative "light curves" (Eddington ratio curves) from different regions of the parameters space. In particular, we emphasize the wide variety of the behaviours for the curves which are consistent with the observed changes in the mean brightness, which is reminiscent of the wide diversity of observed variability behaviours for AGN.

Qualitatively, as indicated before, this model also explains why the most luminous objects are more likely to get dimmer - as they are already occupy the uppermost edges of the probability density function they are far more likely to get dimmer and move to more probable regions of the parameter space. In other words, for the brightest AGN the only way is down!

In future we aim to improve observational constraints and finely map time dependence by incorporating information from different surveys, such as POSS, Pan-STARRS and Zwicky Transient Factory. We also aim to use this full information and luminosity dependence of the effects to place fine constraint on several physical parameters of AGN accretion, in the manner similar as shortly described above.

REFERENCES

Aihara, H., AlSayyad, Y., Ando, M., et al. 2019, arXiv e-prints, arXiv:1905.12221. https://arxiv.org/abs/1905.12221

Astropy Collaboration, Robitaille, T. P., Tollerud, E. J., et al. 2013, A&A, 558, A33, doi: 10.1051/0004-6361/201322068

Bauer, A., Baltay, C., Coppi, P., et al. 2009, ApJ, 696, 1241, doi: 10.1088/0004-637X/696/2/1241

Bland-Hawthorn, J., Maloney, P. R., Sutherland , R. S., & Madsen, G. J. 2013, ApJ, 778, 58, doi: 10.1088/0004-637X/778/1/58

Caplar, N., Lilly, S. J., & Trakhtenbrot, B. 2017, ApJ, 834, 111, doi: 10.3847/1538-4357/834/2/111

Caplar, N., & Tacchella, S. 2019, MNRAS, 487, 3845, doi: 10.1093/mnras/stz1449

Cartier, R., Lira, P., Coppi, P., et al. 2015, ApJ, 810, 164, doi: 10.1088/0004-637X/810/2/164

de Vries, W. H., Becker, R. H., & White, R. L. 2003, AJ, 126, 1217, doi: 10.1086/377486

de Vries, W. H., Becker, R. H., White, R. L., & Loomis, C. 2005, AJ, 129, 615, doi: 10.1086/427393

Edelson, R., Vaughan, S., Malkan, M., et al. 2014, ApJ, 795, 2, doi: 10.1088/0004-637X/795/1/2

Flesch, E. W. 2015, PASA, 32, e010, doi: 10.1017/pasa.2015.10

Fukugita, M., Ichikawa, T., Gunn, J. E., et al. 1996, AJ, 111, 1748, doi: 10.1086/117915

Graham, M. J., Djorgovski, S. G., Drake, A. J., et al. 2014, MNRAS, 439, 703, doi: 10.1093/mnras/stt2499

Gunn, J. E., Siegmund, W. A., Mannery, E. J., et al. 2006, AJ, 131, 2332, doi: 10.1086/500975

Hunter, J. D. 2007, Computing in Science and Engineering, 9, 90, doi: 10.1109/MCSE.2007.55

Ivezić, Ž., Smith, J. A., Miknaitis, G., et al. 2007, AJ, 134, 973, doi: 10.1086/519976

Johnson, S. D., Chen, H.-W., Straka, L. A., et al. 2018, ApJL, 869, L1, doi: 10.3847/2041-8213/aaf1cf

Kawanomoto, S., Uraguchi, F., Komiyama, Y., et al. 2018, PASJ, 70, 66, doi: 10.1093/pasj/psy056

Kozłowski, S. 2017, A&A, 597, A128, doi: 10.1051/0004-6361/201629890

Lawrence, A. 2018, Nature Astronomy, 2, 102, doi: 10.1038/s41550-017-0372-1

MacLeod, C. L., Ivezić, Ž., Kochanek, C. S., et al. 2010, ApJ, 721, 1014, doi: 10.1088/0004-637X/721/2/1014

MacLeod, C. L., Ivezić, Ž., Sesar, B., et al. 2012, ApJ, 753, 106, doi: 10.1088/0004-637X/753/2/106

MacLeod, C. L., Ross, N. P., Lawrence, A., et al. 2016, MNRAS, 457, 389, doi: 10.1093/mnras/stv2997

Miyazaki, S., Komiyama, Y., Kawanomoto, S., et al. 2018, PASJ, 70, S1, doi: 10.1093/pasj/psx063

Morganson, E., Burgett, W. S., Chambers, K. C., et al. 2014, ApJ, 784, 92, doi: 10.1088/0004-637X/784/2/92

Novak, G. S., Ostriker, J. P., & Ciotti, L. 2011, ApJ, 737, 26, doi: 10.1088/0004-637X/737/1/26

Richards, G. T., Fan, X., Schneider, D. P., et al. 2001, AJ, 121, 2308, doi: 10.1086/320392

Rumbaugh, N., Shen, Y., Morganson, E., et al. 2018, ApJ, 854, 160, doi: 10.3847/1538-4357/aaa9b6

Sartori, L. F., Schawinski, K., Trakhtenbrot, B., et al. 2018, MNRAS, 476, L34, doi: 10.1093/mnrasl/sly025

Sartori, L. F., Trakhtenbrot, B., Schawinski, K., et al. 2019, arXiv e-prints, arXiv:1909.06374. https://arxiv.org/abs/1909.06374

Sartori, L. F., Schawinski, K., Koss, M., et al. 2016, MNRAS, 457, 3629, doi: 10.1093/mnras/stw230

Schneider, D. P., Richards, G. T., Hall, P. B., et al. 2010, AJ, 139, 2360, doi: 10.1088/0004-6256/139/6/2360

Shen, Y., Richards, G. T., Strauss, M. A., et al. 2011, ApJS, 194, 45, doi: 10.1088/0067-0049/194/2/45

Smith, K. L., Mushotzky, R. F., Boyd, P. T., et al. 2018, ApJ, 857, 141, doi: 10.3847/1538-4357/aab88d

Vanden Berk, D. E., Richards, G. T., Bauer, A., et al. 2001, AJ, 122, 549, doi: 10.1086/321167

Voevodkin, A. 2011, arXiv e-prints, arXiv:1107.4244. https://arxiv.org/abs/1107.4244